The Use of Satellite Altimeter Data to Estimate the Extreme Wave Climate

CORTIS K. COOPER

Chevron Petroleum Technology Co., San Ramon, California

GEORGE Z. FORRISTALL

Shell International Exploration and Production, Den Haag, the Netherlands

(Manuscript received 3 October 1995, in final form 20 June 1996)

ABSTRACT

Since 1986, nine years of wave data derived from satellites have been accumulated, and this database will expand dramatically in the next two years as two more satellites are added. Several researchers have begun using this data to estimate extreme value statistics for waves. However, one potential problem with satellite data is space–time resolution, which is a poor match for the scales of storms. Satellites only revisit a site once every 10–35 days, and their tracks are separated by 100–200 km. With this coarse sampling, the satellite may miss storms since they have characteristic length and time scales as short as a few hours and tens of kilometers. The purpose of this paper is to explore the impact of this undersampling on the calculated 100-yr wave height. This is accomplished by running Monte Carlo simulations of simplified but realistic storms sampled by a simulated satellite and site. The authors study the sensitivity of the calculated 100-yr wave to variations in storm type, radius, and forward speed; number of satellites; satellite track; and satellite sampling region. The uncertainty, as measured by the coefficient of variation (cov), of the 100-yr wave based on 10 years of satellite data is 10% in regions like the North Sea that are dominated by extratropical storms, provided the satellite data is sampled over a 200–300-km region. This is about the level accepted by present offshore standards like the American Petroleum Institute. For regions dominated by tropical storms like the Gulf of Mexico, the cov for satellite- or site-derived extremes is much greater than 10% using 10 years of data. The situation improves with increased sample period, storm frequency, or the number of satellites. However, even in these cases some caution must still be exercised near the coast where the satellite data itself may be less reliable and sampling over large regions may remove real spatial gradients. Our conclusions apply to all existing satellite tracks including Geosat, Topex/Poseidon, and ERS.

1. Introduction

The feasibility of measuring ocean wave heights from a satellite altimeter was demonstrated by Seasat in 1978, but it has only been in the last few years that enough altimeter wave data has been collected to enable the compilation of climatologies. Data from Geosat (1986–1990), Topex/Poseidon (1992–present), and *ERS-1* (1991–present) are now available. Combined, these represent about nine satellite-years of global coverage. The rate of data accumulation will increase substantially in the near future with the launch in 1995 of *ERS-2* followed in 1996 by Geosat Follow-On. Potentially, this will give four concurrent satellites in operation in the next few years.

The ability of the satellite altimeter to accurately measure wave heights has been demonstrated by several previous studies. Dobson et al. (1987) and Glazman and Pilorz (1990) both compared Geosat wave heights to measurements made by the NOAA National Data Buoy Center and found the Geosat estimates biased 0.4 m lower than the buoy measurements. Carter et al. (1992) reanalyzed this data and concluded that the buoy waves were 13% larger than the altimeter waves. More recently, Cotton and Carter (1994) have compared monthly averages of NOAA buoy data with Geosat, *ERS-1*, and Topex/Poseidon (henceforth referred to as Topex) altimeter measurements sampled over 2° squares. Their regressions showed that the Geosat data adjusted by the formula of Carter et al. (1992) was unbiased compared to the buoys and that

$$H_E = -0.107 + 0.824H_B, \tag{1}$$

and

$$H_T = 0.172 + 0.918H_B, \tag{2}$$

where H_B is the significant wave height from the buoys, H_E is the significant wave height from the *ERS-1* OPR

Corresponding author address: Dr. Cortis K. Cooper, Facilities Engineering Products and Services, Chevron Petroleum Technology Co., 6001 Bollinger Canyon Road, P.O. Box 5045, San Ramon, CA 94583.

records, and H_T is the significant wave height from the Topex Ku band given in the Geophysical Data Records.

Once corrected, the residual scatter between the Geosat and buoy wave measurements studied by Carter et al. (1992) was 0.23 m. The residual rms error for the monthly average ERS and Topex comparisons were both 0.18 m. Comparisons of careful wave hindcasts with measurements (Khandekar et al. 1994; SWIM 1985) show near-zero biases and rms errors from 0.5 to 1.0 m, which translates to less than a 10% coefficient of variation (cov). Ship observations (Hogben and Lumb 1967) require considerable bias correction and have a residual rms error of about 1.3 m. The accuracy of the satellite wave measurements is thus better than either ship observations or hindcasts. This accuracy must be balanced against the long time histories available from ship observations and the high temporal and spatial resolution given by model hindcasts.

Because of their accuracy and global coverage, satellite wave measurements are clearly a valuable resource for the verification and development of wave models. For example, Lefevre et al. (1994) compared altimeter measurements from the first year of the Topex/Poseidon mission to the French operational wave model for the North Atlantic and found that the model was unbiased. The best wave global hindcasts and forecasts should ultimately come from numerical models into which satellite measurements have been assimilated.

It is clear that satellite altimeters provide a large and growing database of accurate wave measurements on a worldwide grid. Despite these virtues, engineers have been slow in using the data. This is due, in part, to the fact that the sampling pattern of satellite altimeters has been optimized for studies of ocean circulation rather than wave heights. A satellite altimeter cannot map a storm wave field well because atmospheric storm systems move much faster and have much shorter durations than most oceanic circulation features. In addition, tropical storm systems are very small compared to typical distances between altimeter tracks.

Figure 1 illustrates the mismatch between the altimeter sampling pattern for Geosat and a severe hurricane in the Gulf of Mexico. The altimeter tracks are separated by roughly 100 km and the pattern is repeated only every 17 days. The small circle in the figure shows the radius to maximum wind in Hurricane Camille. Since the forward speed of Camille was 15 km h^{-1}, it remained in the gulf only a day. Geosat crossed the gulf just once or twice a day with a typical distance between crossing of several hundred kilometers. Clearly, the odds of Geosat measuring the near-maximum waves in a hurricane are not good. The sampling patterns of other satellites such as *ERS-1* and Topex/Poseidon are no more likely to capture the highest waves in a small storm.

Although a satellite altimeter cannot produce a detailed map of the waves in a storm, the data can be used to estimate the statistical properties of the wave climate if it averaged over a reasonable area. Increasing the sampling area will improve the statistical stability of the estimates and increase the chances of sampling the highest waves in a storm, but increasing the area also has drawbacks. If the area is too large, real spatial variations in regional wave heights caused by climate or bathymetry will be obscured. Finding the proper balance between stability and resolution is a common problem in statistics. For example, Chouinard (1992) did a statistical analysis of hurricane wave hindcasts in the Gulf of Mexico and found that the optimum length scale for smoothing the results was 150 km.

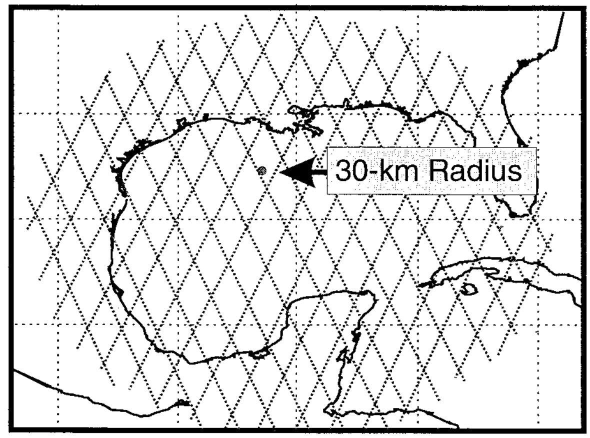

FIG. 1. Geosat satellite repeat paths for the Gulf of Mexico. Small circle indicates the radius to maximum wind of a typical TS.

The primary purpose of this paper is to examine the errors in design wave heights due to the sampling patterns of satellites. Previous studies of the effects of the sampling pattern of satellite altimeters have focused on ocean current processes with much longer length scales and much slower translation speeds than wave-generating storms. For example, Kindle (1986) and Hogan et al. (1992) looked at sampling ocean eddy fields and permanent currents. They found the satellite altimeter could adequately sample oceanic mesoscale features characterized by length scales of order 100 km and translation speeds of order 3 km day^{-1}.

Efforts to use satellite-derived waves have touched on space–time sampling issues. Tournadre and Ezraty (1990) compared wave height statistics derived from Geosat measurements for different-sized regions surrounding the Frigg platform in the North Sea. Tests on statistical consistency showed that the wave heights belonged to the same statistical population out to a radius of 200 km, except that the statistics for a 50-km radius were different due to "undersampling." They also found that 50-yr extreme wave heights derived from satellite data were in good agreement with site data if the satellite data were sampled over 100–200-km-radii regions.

Other studies also suggest that a 200-km sample region seems to work reasonably well at least for regions dominated by large-scale storms. Charriez et al. (1992) sampled Geosat data over a 200-km radius near three sites: at the Frigg platform (North Sea), Palanca (West Africa), and the English Channel entrance. They found extreme values compared well with those derived from in situ data. Carter (1993) found similar results for the entire North Sea except for coastal regions, where the Geosat had difficulty because of the well-known ''land shadow'' effect.

Young (1994) produced maps of the monthly mean wave height in $4° \times 4°$ squares from three years of Geosat data. He compared probability distribution functions of the mean and maximum wave heights in a square with buoy measurements from a southern ocean site. The distribution of the means was lower than the buoy distribution function and the distribution of the maxima was higher than the buoy distribution. We will show below that using all of the satellite measurements from each pass in the calculation of the distribution function is more consistent with standard interpretations of the statistics of measurements at a site. Young (1994) also produced maps giving wave heights at 10%–90% exceedence levels based on the distribution functions for the means in the satellite passes but remarked that ''extrapolation of the relatively short 3-yr data set to extreme events is likely to be unreliable. . .''

In summary, previous investigators who have calculated extreme criteria from altimeter-derived waves have sampled over radii of 100–200 km. This size is based largely on intuition and tested in regions dominated by extratropical storms with large characteristic length scales.

The purpose of this paper is to look carefully at how the space–time limits of altimeter-derived data can impact extreme wave height estimates. To concentrate on the effects of spatial averaging, we assume that the measurements are perfect. We do not consider the bias in satellite extremes due to measurement error, as this has already been studied extensively by Cotton and Carter (1994) and others listed above. We look at small-scale (20 km) tropical and large-scale (500 km) extratropical storms. Our approach is to use Monte Carlo simulations of storms sampled by synthetic satellites. By using simulations, we can eliminate instrument error effects and repeat the same climate many times in order to obtain precise statistics. Our approach is similar to Mestas-Nunez et al. (1994) who studied the effect of the Seasat sampling scheme on average wind stress fields.

In the next section we start with a simple deterministic case. We evaluate the ability of the altimeter to measure extremes in storms of various radii, translation speeds, and with different-sized sampling regions. Storm intensity is fixed but the storm path is varied randomly. Altimeter results are compared to a site and perfect data. The third section explores statistical issues. We derive extreme statistics for storm intensities and sizes typical of two regions: the Gulf of Mexico and the North Sea. Our results explore the sensitivity of extreme statistics to sample region. Again we compare results from the altimeter to site data. The fourth, and final section, summarizes our findings, which include recommendations for the spatial averaging that should be used in estimating wave climate statistics from altimeter measurements.

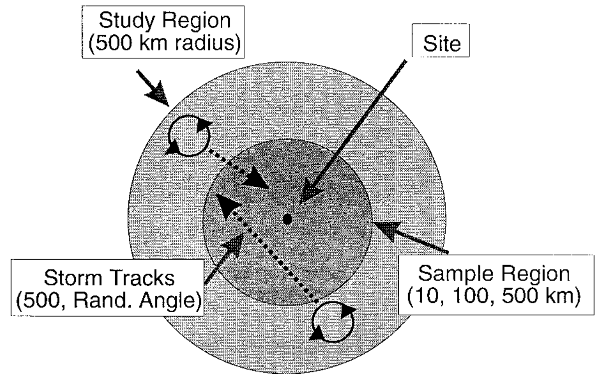

FIG. 2. Schematic of the deterministic experiment. Storms are released at random over the larger circle; satellite samples are taken over the inner circle; site samples are taken at the center of the circle.

2. Deterministic case

The purpose of this case is to assess the ability of the satellite altimeter to measure a variety of storm systems. Storm wave fields are modeled using simple parametric equations. Five hundred randomly released storms with fixed intensity are sampled. We compare the satellite to site data. Satellite measurements are derived by sampling the storm fields from a ''perfect'' altimeter flying along known satellite paths with a randomly selected phase shift. We study the sensitivity of the result to changes in storm radius, storm forward speed, sample region, storm duration, and satellite track configuration.

a. *Methodology*

Figure 2 shows a schematic of the experiment. A storm of constant forward velocity, radius, and intensity is released at a randomly selected distance and angle relative to a central site. The storms travel in a straight line and can start anywhere so long as they reach their midpoint somewhere within the study region of radius 500 km. Five hundred storms are released at a random time relative to the satellite track passage at the center site. Sensitivity studies show that 500 storms are sufficient to provide stable statistics.

Satellite measurements are based on data collected from any track passing through the interior circle or sample region. The size of the sample region should be dictated by the expected spatial and temporal variations in the wave field due to physical processes. Such variations would most commonly be evident near the coast where fetch limitations or shallow-water effects could cause substantial spatial gradients in the wave field. Reasonable values for a sample region would range from near zero at a shallow site near a complicated coast, to greater than 500 km in an open sea region dominated by large-scale storms.

The study region should depend on the coherence scale of the storm population. In other words, storms passing outside this region are assumed to come from a different storm population and should not be included in the storm statistics for the site of interest.

We measure the success of a method by counting the number of storm "hits" and "misses" from each method. More specifically, if the satellite or site records a wave height that is 75% of the maximum in the storm, then it is a "hit," otherwise it is a "miss." Results are normalized to remove a number of factors including storm intensity, hit threshold (75%), and storm radius R_{max}. It can be argued that a high-quality model hindcast provides a "perfect" measurement in our study. This is because we only consider errors due to space–time sampling bias. Theoretically, this error in a model should be negligible if the grid size and time step are properly selected.

The fixed parameters in our experiment are the number of storms in the Monte Carlo simulation, the study region size (500 km), and storm intensity. The variable parameters are storm type (tropical or extratropical), storm radius, storm forward speed, storm duration, sampling region, and satellite type.

To generate the storm wave fields, we use previously published parametric models. Tropical storm (TS) wave fields are based on Cooper (1988) or

$$W_{max} = 0.885(5.6\sqrt{\Delta P} - 0.5R_{max}f) \tag{3}$$

$$H_s = 0.25W_{max}\left(\frac{r}{R_{max}}\right)^{-0.38}, \tag{4}$$

where r is the distance from the center of the storm (always greater than R_{max}), ΔP is the central pressure, f is the Coriolis parameter, R_{max} is the radius to maximum winds, W_{max} is the maximum wind in the storm, and H_s is the significant wave height. All units are mks (meter, kilometer, second) except ΔP, which is in millibars. These equations have neglected the angular dependency in Cooper (1988)—we assume the storms are axisymmetric. This should have no impact on our final results because of the way in which we normalize. We do not have to worry about specifying the region $r < R_{max}$. This is because simple geometric constraints mean the site or satellite will always see values at R_{max} if it passes inside R_{max}. It follows that since we are only interested in the maximum seen then we only need the value at R_{max}.

Extratropical storms (ETS) are modeled with the wind field suggested by Stone and Webster Engineering Corp. (1978). They analyzed eight ETSs off the coast of New England and developed the following equations:

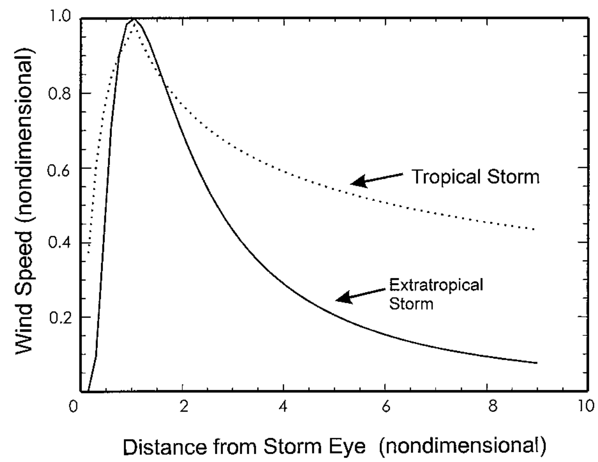

FIG. 3. Nondimensionalized cross-sectional wind (or wave) profiles for the TS and ETS models.

$$P = \Delta P \exp\left(\frac{-2R_{max}}{r} + 0.73\right) \tag{5}$$

$$W_s = \left(\frac{0.1P}{f\rho_w}\right)\left(\frac{R_{max}}{r^2}\right), \tag{6}$$

where P is a local pressure term at a distance r from the storm center, ρ_w is the density of air, and all other terms are as defined in (3). The geostrophic wind expression has been applied and the constant tuned to give roughly a 1-h wind at 10 m. The constant is of little consequence because of our normalization process.

Stone and Webster Engineering Corp. (1978) did not calculate wave height, so we assume that the wave height is proportional to wind speed ($H_s = 0.25W_s$). Again, the exact proportionality factor is unimportant because we measure the success of the satellite relative to a site—in essence, we normalize the result. Our assumption of proportionality is consistent with the findings of Cooper (1988) for TSs. For ETSs, Peters et al. (1993) found wave and wind time series at a site to be highly coherent near the storm peak. This suggests there will be a high degree of spatial coherence between wind and wave.

Figure 3 shows the cross-sectional profiles of the two models as a function of the normalized distance from the center of the storm. The mean radius to maximum waves (or winds) for the ETSs is a factor of four greater than for TSs.

Satellite measurements are derived by sampling the storm fields from a "perfect" altimeter flying along known satellite paths with a randomly selected phase shift. Measurements are only taken when the pass is within the sampling region in Fig. 2. Site measurements are based on a sample taken every hour. Satellite samples are taken every second, corresponding to a 7-km increment along a track.

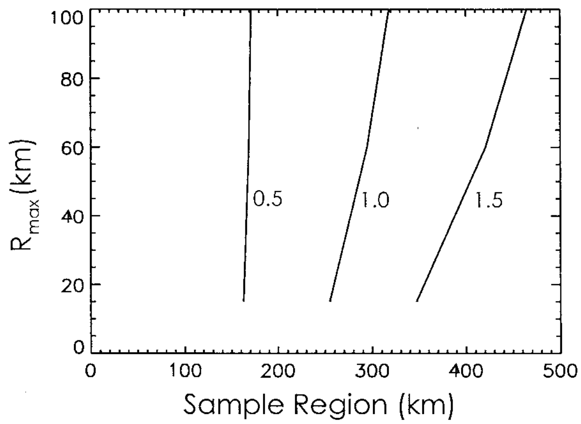

FIG. 4. Site ratio for the TS base case. Storm is moving 2.7 m s^{-1} and lasts for 3 days (means for the gulf). Satellite samples are based on Geosat paths (17-day ERM).

b. Results

Figure 4 shows contours of the site ratio for various storm and region radii. Recall the site ratio is simply the number of satellite hits divided by the number of site hits. The figure is for the base case TS with a forward speed of 2.7 m s^{-1} and duration of 3 days assuming a Geosat orbit. These are the mean storm characteristics for Gulf of Mexico TSs. The 3-day duration assumes the central pressure remains within 75% of the minimum recorded during the storm. The storm duration is inversely proportional to this cutoff. A cutoff of 75% was selected somewhat arbitrarily, although it is clear some cutoff is needed to prevent samples when the storm is atypically weak. In the gulf, the mean storm would travel 650 km or of order half the length of the gulf.

Table 1 shows the data upon which Fig. 4 is based. The first column shows the storm radius (km), the second (third, fourth) column shows the number of satellite hits for a sample region of 10 (100, 500) km, and the fifth column shows the hits for the site. Figure 4 is developed by dividing columns 2–4 by column 5.

The radii in the table and figure are based on storm statistics in the gulf—a mean radius of 58 km with a standard deviation of 46 km. Similarly, the forward speed and duration for the base case are the mean values for the gulf: a mean (standard deviation) for forward speed is 2.7 m s^{-1} (1.3) and a mean (standard deviation) for duration of 70 h (15). Our experience with TSs in other areas, such as the South China Sea and Northwest Australian Shelf, suggest their characteristics are similar. Any differences are well within the range of the sensitivity results included below.

The sample regions used in the table and figures are based on what we would consider a reasonable range. The 500-km sample region corresponds to open sea conditions where the storm population is homogenous over large length scales. The 10-km sample radius corresponds to near-coastal sites where fetch and shallow-water effects cause large gradients in the local waves.

TABLE 1. Summary of hits for satellite and site for mean TS (forward speed of 2.7 m s^{-1}, duration of 3 days). The total possible number of hits is 500.

	Sample region (km)			
R_{max} (km)	10 km	100 km	500 km	Site
15	0	5	73	35
60	8	31	246	140
100	17	55	346	220

Figure 4 compares the satellite measurements to those seen at a site. The larger the ratio the better the satellite performs relative to site measurements. The region to the right (left) of the "1.0" contour indicates the satellite (site) is superior to the site (satellite). As expected, the satellite performance improves rapidly relative to a site as the satellite sampling region increases. Another obvious feature is the positive contour slopes for larger sampling regions. These are two dominant features of all the subsequent results as well, and they will be discussed below.

In general, Fig. 4 shows the satellite performs about equally to site data if the satellite data is sampled from a 280-km region regardless of storm radius. As expected, the situation improves as the storm slows down and lasts longer. Table 2 shows the case for a storm moving at 1.5 m s^{-1} and lasting 4 days. The number of satellite hits for the 60/100 (storm radius/sample region) case increases by nearly 70% from the base case. A closer look at other results not shown here suggests that the change in speed and duration contribute equally. Note that changing the translation speed and duration characteristics does not appreciably affect the number of site hits. In other words, the last column of Tables 1–3 is constant.

Satellite performance deteriorates substantially for fast-moving, short-lived storms. Table 3 shows the case for a storm moving at 4.0 m s^{-1} and lasting 2 days. The number of satellite hits is cut by over one-half for the 60/100 case. Similarly, the sampling region needed to achieve parity with a site for the mean storm radius increases by almost 200–470 km. A closer look at results not shown here shows that 75% of this comes from the decrease in storm duration.

Regardless of the storm characteristics, neither the

TABLE 2. Summary of hits for satellite and site for slow-moving (1.5 m s^{-1}), long-lived (4 days) TS. The total possible number of hits is 500.

	Sample region (km)			
R_{max} (km)	10 km	100 km	500 km	Site
15	0	11	92	35
60	16	50	300	140
100	29	106	406	220

TABLE 3. Summary of hits for satellite and site for fast (4.0 m s^{-1}), short-lived TS (2 days). The total possible number of hits is 500.

	Sample region (km)			
R_{max} (km)	10 km	100 km	500 km	Site
15	0	3	58	30
60	3	13	162	140
100	6	46	247	220

satellite nor a site performs nearly as well as a model potentially can. This can be seen by comparing columns 2–5 of the previous tables with the number 500, which is the number of hits that a model would see. Only in the best-case scenario of large sampling region and large storm radius does the satellite begin to approach a model (406 vs 500). Even for large storms, a site sees less than one-half the hits a model would. Of course these statements assume a model uses adequate space and time resolution and is calibrated to be unbiased. Previously mentioned work suggests carefully constructed models can satisfy these assumptions.

The satellite and site both perform better for ETSs. Table 4 shows the results for an ETS based on the mean characteristics of 53 storms in the northwest Atlantic compiled by Stone and Webster Engineering Corp. (1978). As a whole, these storms have a mean radius and forward speed about four times larger than TSs. Because the ETSs tend to move so fast their peak duration is shorter than TSs. The site performs well even for relatively small storms. For storm sizes near the mean or larger, the site is nearly perfect. The satellite compares well with the site for even smaller storms if a sampling region of about 200–300 km is used.

We have also briefly investigated the influence of the satellite characteristics by running two cases with one ERS satellite, and two satellites (*ERS-1* and Topex). *ERS-1* has a repeat path of 35 days so it has almost double the space resolution of Geosat, but one-half the time resolution. Topex has a 10-day repeat path. The single ERS case performs almost identically to Geosat, and results are not shown here.

The joint *ERS-1*/Topex case performs substantially better than the Geosat case, as can be seen from a comparison of Table 5 and Table 1. Ignoring the cases where there are less than 20 hits, we see that *ERS-1*/Topex sees an average of 60% more hits than Geosat alone. The joint *ERS-1*/Topex is especially interesting since the two have been flying together since 1993.

TABLE 4. Summary of hits for satellite and site for mean ETS. The total possible number of hits is 500.

	Sample region (km)			
R_{max} (km)	10 km	100 km	500 km	Site
125	3	39	292	228
250	19	126	469	466
375	36	222	496	500

TABLE 5. Summary of hits for satellite and site for mean TS sampled by *ERS-1* and Topex satellites. The total possible number of hits is 500.

	Sample region (km)			
R_{max} (km)	10 km	100 km	500 km	Site
15	2	6	176	43
60	11	56	385	130
100	18	84	451	205

c. Discussion

One dominant feature in the results is the linear increase in the site ratio with sampling radius. Figure 5 demonstrates this trend and is based on a run with a fast-moving TS of 2-day duration. Though there is some scatter, the linear trend is apparent. The reasons for the linear trend are as follows. First, we note that the denominator of the ratio (site hits) is independent of the sample region size so changes in the ratio are due to changes in the number of satellite hits. The latter will increase in proportion to the number of tracks crossing the sample region. In other words, if we double the sample region radius, this doubles the number of track crossing and hence doubles the chance of getting a hit, all else being equal.

Another dominant feature in the results is the diminishing performance of the satellite for larger-scale storms at larger sample regions, that is, the positive slope evident in Fig. 4 at larger sampling radii. The behavior is also apparent in Fig. 5 in the form of a nonlinear ‘‘leveling’’ of the data for the larger storm and sample radii. The reason for this behavior is due to a truncation or ‘‘cutoff’’ effect imposed by the outer boundary, that is, the study region in Fig. 2. To see this, imagine that 10% of the storm population are what we will call peripheral storms that pass over 450 km from the center. A large portion of a peripheral storm will lie outside the study region and so can never be sampled

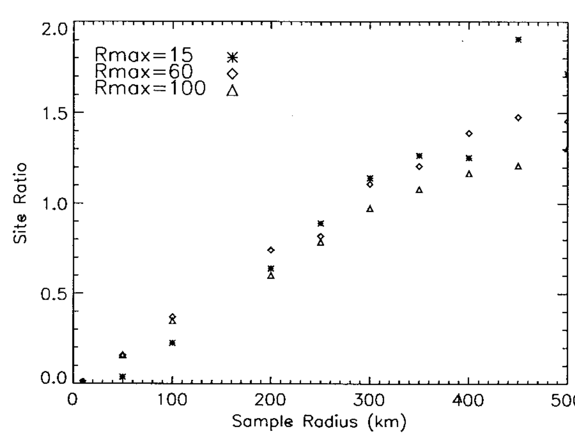

FIG. 5. Site ratio versus sample radius for a fast-moving TS with short duration. Note the tendency for a linear increase in site ratio modified by a leveling trend for larger sampling and storm radii.

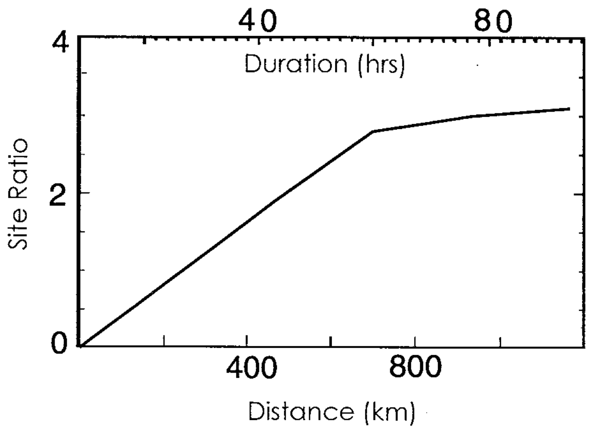

FIG. 6. Site ratio versus distance traveled by a storm during its life. Results are for a TS moving at 2.7 m s^{-1} (mean). Note how site ratio levels as total distance traveled reaches the sample region size of 500 km.

by the satellite no matter how large the sample region. Furthermore, the larger the storm, the larger the area that lies outside the study region and so the smaller the odds the satellite will see the storm. These peripheral storms will not affect the satellite results for smaller study region sizes, but as this increases the effect becomes more pronounced.

Another interesting feature is the strong tendency of the satellite performance to level off for faster, longer-duration storms. This is evident if one closely compares Tables 1–3. Figure 6 demonstrates this asymptotic behavior for a TS traveling at 2.7 m s^{-1} in a 500-km sample region. The change in the site ratio is nearly linear when the total travel distance is much less than the sample region. However, as the travel distance increases, the ratio changes much more slowly. There are two factors that cause this. The shorter distances are dominated by the tendency for performance to increase as the storm duration increases. For a stationary storm, this increase will be linear. However, the storms are not stationary and some may travel outside the sampling region before the satellite passes. Hence, as the total travel distance of the storm exceeds the sampling region radius, the gains in satellite performance drop off rapidly.

We can also draw some preliminary conclusions regarding the ability of a site or satellite to measure various types of storms. Based on the above results, it seems that neither the satellites nor sites are well suited to measuring TSs, particularly in regions where storms are infrequent. For example, in the Gulf of Mexico where there is about one TS per year, a site will be hit by the average storm about once every 4 years. For small storms like Camille, the average sample rate becomes a dismal 14 years. The satellite measures even fewer storms than the site if the sample radius is less than 250 km.

Satellites look much more promising for ETSs than TSs. This is due to the larger storm sizes and the smaller distance between satellite tracks at higher latitudes where ETSs are found; for example, at 50° latitude, the tracks are 20% closer than at 20°. For mean storm conditions, the number of satellite hits (250) in ETSs is more than double the number for TSs (111) using a 250-km sample region. While this is only one-half that seen at a site, it is still a substantial number of samples. We can also expect extreme analysis of satellite data to be relatively good since ETSs tend to occur frequently.

3. Stochastic case

The purpose of this case is to assess the accuracy of extreme values derived from a satellite altimeter for various storm systems and sampling region sizes. As in the deterministic cases, a parametric wind model is used. But unlike the deterministic case, the storm parameters (forward velocity, radius, and intensity) are varied in time. To obtain stable statistics, we run 25 realizations of the storm histories. Each realization uses the same storm parameters, but with different random tracks and directions.

Cumulative probability distribution functions (CDF) are developed for the site and for the different satellite sampling regions. The extremes of the CDFs are fitted with a Weibull distribution function. The mean and standard deviation of the 100-yr return values are then compared between the site and satellite results.

a. Simulations

The experiment follows the same strategy depicted in Fig. 2 and used in the deterministic experiments, except that the storm intensity, radius, and forward speed are taken from databases of actual storms. For TSs we use parameters from the National Climatic Data Center (NCDC) data tape TD-9636. We selected the 100 most severe storms from 1900 to 1990 that passed within 200 km of the central Gulf of Mexico.

For ETSs, the storm population comes from two databases. The storm radii are based on Stone and Webster Engineering Corp.'s (1978) parametric fits of 54 ETSs that occurred in the western North Atlantic from 1944 to 1976. The central pressure and forward speeds come from NCDC TD-9636. We selected all storms that passed within 500 km of 60°N, 1°E in the North Sea during 1966–85. This selection process produced 572 storms. Spurious low pressures that occurred during several of these storms were edited out. A single value of pressure and translation speed is used because a brief review of the NCDC archives suggests the storms are reasonably constant over these distances. It would have been preferable to use only one of the two databases, but Stone and Webster had insufficient storms, while NCDC did not include storm radius. Mixing storms from the western and eastern North Atlantic is justified since the eastern storms tend to originate from the western North Atlantic.

We develop 572 ETSs using the NCDC pressure–velocity data randomly combined with the radii from Stone and Webster. This assumes that there is no correlation between translation speed, intensity, and radius. This appears reasonable based on the low correlations in the 54 Stone and Webster ETSs, that is, correlation coefficients of 0.4, −0.007, and 0.005 between radius–pressure, radius–speed, and pressure–speed.

As in the deterministic case, the storm path remains random. The storms travel in a straight line and can start anywhere so long as they reach their midpoint somewhere within the study region in Fig. 2. For TSs, the central site in Fig. 2 resides at roughly the geometric center of the gulf—26°N, 90°W. All of the hurricanes pass within 200 km of this location.

Twenty-five realizations of the storm histories are run, where each realization uses randomly selected paths. The tracks are randomized primarily because of the limited number of historical TSs in the Gulf of Mexico. Work by Chouinard (1992) and others show that there is considerable spatial variability in the site extremes in the Gulf of Mexico. While there may be some physical basis for this variability, it may be a result of the limited number of severe storms in the database. For this experiment, we assume the latter is correct and eliminate any spatial variability by making all tracks equally likely. Eliminating the spatial variability is beneficial to the satellite. This is because the spatial variability has a scale on the order of 100 km and the satellite would have difficulty resolving these scales—a fact clearly demonstrated by our deterministic experiment.

Satellite measurements are derived by sampling the storm fields from a ''perfect'' altimeter flying along known satellite paths with a randomly selected phase shift. One of the satellite tracks passes over the site—the other tracks are spaced at the interval appropriate for the specific satellite and latitude. Measurements are only taken when the pass is within the sampling region in Fig. 2. Site measurements are based on a sample taken every 2 h. Satellite samples are taken every 1 s, corresponding to a 7-km increment along a track.

In each realization, the satellite sees the same storms that are measured by the site. Differences between the satellite and site measurements are thus due solely to the sampling pattern of the satellite.

In the discussions below, we compare the uncertainty of the various estimates from the satellite and site. We often label a cov of greater than 10% as unacceptable for engineering design. This comes from two sources. First, offshore design standards for many regions are now based on hindcast models, for example, the Gulf of Mexico (API 1993), which have near-zero bias and a cov of less than 10% for more severe, design-level storms (Khandekar et al. 1994; SWIM Group 1985). Second, design standards in the North Sea (DOE 1987) allow design waves based on 3–5 years of site data. Our analysis (below) shows site data of this length in the North Sea has a cov of roughly 10%.

b. Distribution functions

The method of producing extreme values from satellite measurements deserves some discussion since the sampling pattern is so different from the time series data from which extreme values are usually calculated. The simplest method of estimating extreme wave heights is through the CDF. The CDF is the probability that a random wave measurement will be less than h. Given a time series of wave measurements, the CDF is estimated as the fraction of the observations that are less than h. Note that the sampling rate has no effect on the expected value of the CDF. If, for example, the sampling rate is increased so that the total number of samples is doubled, the number of samples less than h will also be doubled. Similarly, the expected value of the CDF is not changed if the observations from two sites that experience the same wave climate are combined. This point is not generally appreciated, and a familiar example may make the argument clearer. Consider a time series of band-limited white noise, such as a recording of the wave elevation at one point. The theoretical distribution function of such a time series is Gaussian if the waves are linear, and the expected value of any sample distribution taken from the series is also Gaussian, no matter what the sampling interval.

The satellite measurements can be thought of as observations made at hundreds of sites at an interval of several days; 17 in the case of Geosat. If the wave climate at all the sites is the same, as it is in our simulations, the observations from the sites can all be combined to make a single CDF that has the same expected value as the CDF of observations at a single site that samples continuously. Although the expected values of the CDFs constructed in this way are equal, sampling variability will cause each realization of the CDF to be different. The purpose of our simulations is to estimate the size of this variability as a function of the size of the satellite sampling region.

The measurements from the site and satellite passes are sorted into bins of 0.25-m width for all storms within a realization. Results are binned not only for the site but for four sampling regions: 10, 100, 300, and 500 km. From this binned data, CDFs are constructed for each realization. We do not simulate continuous time series of measurements at either the site or along the satellite track, but we assume in calculating the CDFs that the storm simulations capture all of the high wave tails of the distributions.

The plotting probability for the CDF depends on the data source. In the case of site data, the probability of a single simulated significant wave height is the reciprocal of the number of 2-h sample intervals in the y years of the simulation. The count of waves exceeding a given level is thus divided by $(24/2) \times 365.25 \times y$ to get the probability. For the satellite, the counts are divided by $d \times 365.25 \times y$ where d is the number of satellite measurements per day in a given region. For

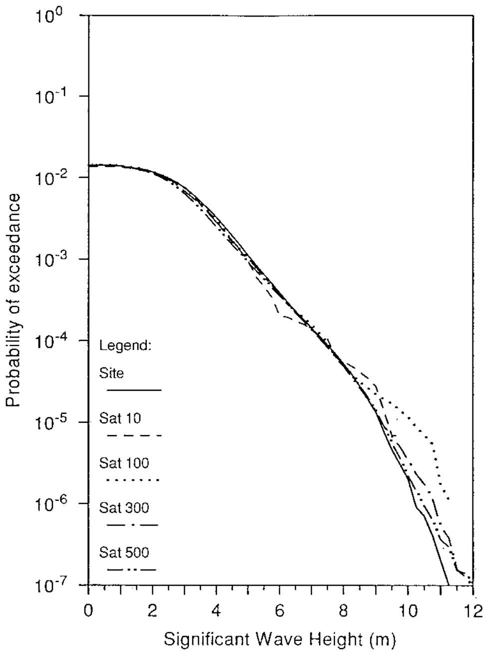

FIG. 7. Probability of exceedence for 25 realizations of 90 years of TSs for various sample regions.

example, $d = 103.3$ for the 500-km sample region at the TS latitude of 25°. For the ETS latitude of 50°, $d = 161.5$ for the 500-km sample region. The number of measurements in other sample regions scales roughly as their radius squared.

Figure 7 shows the CDFs constructed by combining all 25 realizations of the 90 years of TS simulations. Combining the 25 realizations gives good estimates of the expected values of the distributions down to rather low probability levels. The expected value of the distributions from the satellite data are clearly the same as the distribution from the site data, but the satellite datasets for the smaller sampling regions are small enough that noticeable sampling variability remains even when all the realizations are combined. The distributions begin at about 10^{-2} since TSs are only present about 1/100 of the time.

c. Extreme values

To quantify the variability of the CDFs in practical terms, we fit extreme value distributions to them and estimated 100-yr wave heights from the fitted distribution. The sample CDFs were fit to the Weibull three-parameter distribution,

$$P(H_s > h) = \exp\left[-\left(\frac{h - \theta}{A}\right)^B\right]. \quad (7)$$

The three parameters of the distribution, A, B, and θ were found using the maximum-likelihood method with an iterative search over θ. Only wave heights greater than 3.75 m were used in the fits since only high waves in storms appear in the simulations. In a real extreme value analysis, the type of distribution used, the fitting method, and the lower limit of the data used would all be the subject of considerable scrutiny, but for our purposes, it is only important that a representative and robust method be used for all of the different datasets.

Equation (7) gives the probability that a randomly chosen significant wave height will exceed h. The 100-yr wave height is the wave height at which the Weibull distribution has a value of

$$P = \frac{L}{24 \times 365.25 \times 100}, \quad (8)$$

where the denominator is the number of hours in 100 years and L is the decorrelation timescale for the wave height time series (Tucker 1991). Note that L is not necessarily the sampling interval, although it is often taken as 3 h, which is also a common sampling interval for significant wave heights. Clearly, since the expected values of the CDFs are the same for the site and satellite data, the probability level for the 100-yr wave height should be the same for either data source. The sampling rate of the satellite has no logical connection with the value of L. We used $L = 3$ h in our calculations, although that is probably a bit shorter than the true decorrelation scale. Again, this assumption does not affect the comparisons between the sampling methods.

TABLE 6. The 100-yr significant wave heights from 90 years of TS simulations.

Region	Mean (m)	cov (%)	Combined (m)
Site	10.05	9.6	10.11
Sat 10	12.47	98.7	10.50
Sat 100	10.40	25.8	10.96
Sat 300	10.16	9.3	10.22
Sat 500	10.38	4.1	10.41

d. Results

The statistics of the extreme value calculations for 90 years of TS simulations are given in Table 6. The column labeled "mean" gives the average of the 100-yr wave heights estimated from the 25 simulations. The column labeled cov is the coefficient of variation or the standard deviation divided by the mean. It gives a convenient measure of the variability of the estimates. The last column gives the mean 100-yr wave height estimated from the CDF of all 25 simulations combined. The combined mean from 25 realizations of the storms at a site is equivalent to an estimate from 25 measurement points spread through the region of interest.

Subsequent discussion focuses on the cov, not the means. Comparing the means in the tables would be somewhat fruitless since the means include uncertainty due to sampling as well as the extremal analysis (e.g.,

TABLE 7. The 100-yr significant wave heights from 20 years of TS simulations.

Region	Mean (m)	cov (%)	Combined (m)
Site	10.09	15.3	10.21
Sat 10	9.84	84.3	11.66
Sat 100	10.52	54.9	10.70
Sat 300	10.05	13.0	10.35
Sat 500	10.22	7.3	10.34

TABLE 8. The 100-yr significant wave heights from 20 years of ETS simulations.

Region	Mean (m)	cov (%)	Combined (m)
Site	16.13	4.9	16.19
Sat 10	17.02	24.3	16.74
Sat 100	16.98	20.2	16.27
Sat 300	16.71	9.0	16.71
Sat 500	16.32	7.4	16.34

the goodness of the Weibull fit). It would be equally fruitless to strictly benchmark the means in the table to some ''standard'' such as the API (1993). This is primarily because the API used much more sophisticated hindcast models.

The cov of the estimates in Table 6 decreases as the size of the region increases. The cov is very large for the 10-km radius of satellite data since the extreme value fit is made over very few measurements. The satellite makes less than 100 measurements of significant wave height at its 7-km resolution in a simulation of 100 tropical storms over 90 years. On the other hand, the cov for satellite data collected over a 300-km radius is close to the cov of the 100-yr wave heights for site data. This result is consistent with the results in Table 1, which shows that the number of storms measured by the satellite equals the number measured at a site when the radius is about 300 km.

Table 6 demonstrates how the uncertainty of the extreme wave height estimates varies with the sample region, but it is unrealistic since it will be a long time before 90 years of either site or satellite data can be collected. Table 7 shows the statistics of the 100-yr wave height for a more realistic 20 years of TS simulations. The table shows results for the first 20 years in the TS database. Since the storm parameters for this 20-yr period are a subset of the 90-yr dataset, the expected value of the 100-yr wave heights should not necessarily be the same, although they actually turned out to be close. Calculations with other 20-yr subsets produced somewhat different 100-yr wave heights, but similar cov values.

Clearly, the uncertainties for the 10- and 100-km sampling regions are much larger than the roughly 10% cov from good hindcast models that are typically used for final engineering design. The 13% cov for the satellite data from the 300-km radius is a bit better than the site cov (15%), although both of them are marginal for engineering use. The cov for satellite data from a 500-km radius is quite respectable, but it is unlikely that storm characteristics are actually ever homogeneous over such a large region. Table 7 reminds us that it is difficult to collect enough data on Gulf of Mexico TS waves for extreme value analysis even from a continuously operating site. This difficulty is one of the main reasons why design criteria standards in the gulf are based on wave hindcast models that can include much longer sample periods. However, the satellite and site should fare better in other TS-dominated regions where storms are more frequent such as the South China Sea.

Table 8 gives the statistics of the 100-yr wave height estimates for 20 years of simulated ETSs. The cov of the site data is small (5%), in agreement with the use of such data for setting criteria in areas such as the central North Sea where long series of measurements exist. The cov's from the satellite estimates are all larger than the cov at the site, although the 300- and 500-km cov's are under 10% and quite usable for final design. Table 4 shows that the 500-km-radius satellite data gets samples from nearly all of the storms, but the tail of the 500-km CDF still shows more variability than the CDF from the site, presumably because of variability in the length of the satellite track over the few most severe storms.

It is interesting to compare the cov from the TSs and ETSs. For the smaller sampling regions, the ETS cov is substantially smaller than for TSs, as one might expect from the deterministic experiment that showed the satellite got many more hits in ETSs than TSs. However, as the sample region grows, the cov's from the two storm types becomes increasingly similar. There are two reasons for this. First, we see from comparing the 100- and 500-km columns in Tables 1 and 4 that the ratio between ETS and TS rapidly decreases as the sampling region increases. Second, the cov of the sample distribution depends on the number of hits. If there are a factor of r fewer hits, a given cov of the sample distribution appears at a probability level r times higher. This cov is then extrapolated out, roughly linearly on a semilogarithmic plot, to the 100-yr level. The 100-yr cov is thus roughly proportional to the inverse of the logarithm of the number of hits. The final result is that the cov of the two storm types tends to converge for large sample regions.

Since there is at most 5 years of data available from any given satellite (and only 9 years total), it is of interest to look at the uncertainty of estimates based on less than 20 years of data. Table 9 shows the result for 5 years of data for gulf TSs. There were so few measurements in the 10-km radius that many of the extreme value fits did not converge. The cov's for the larger sampling regions increase by about a factor of 3 from the 20-yr cov's, and the site cov increases by a factor of 4. In general, the cov's are too large to be of much use. The situation is actually somewhat worse than indicated in the table because the uncertainty becomes a

TABLE 9. The 100-yr significant wave heights from five years of TS simulations. The asterisk indicates that many of the extreme value fits did not converge.

Region	Mean (m)	cov (%)	Combined (m)
Site	10.28	62.0	10.23
Sat 10	*	*	15.75
Sat 100	9.08	58.8	12.13
Sat 300	10.76	30.8	10.67
Sat 500	10.28	19.6	10.05

TABLE 11. The 5-yr significant wave heights from five years of TS simulations derived from *ERS-1*/Topex data.

Region	Mean (m)	cov (%)	Combined (m)
Site	10.08	57.7	10.25
Sat 10	*	*	7.54
Sat 100	7.93	41.2	9.38
Sat 300	10.37	22.9	10.25
Sat 500	10.23	13.7	10.35

strong function of exactly which five years are included. For example, for another 5-yr period that we modeled, we found the 100-yr mean for the 300-km radius to drop by over a meter.

In contrast, one can still get reasonable statistics for ETSs from five years of data. Table 10 shows the results. The cov increases from the 20-yr but only by about 30%. For the site and 500-km sample region, the cov remains at 10% or less. The 300-km sample is 12%, which is still probably acceptable even for final design. One bit of bad news is the fact that the mean for the satellite extremes from the 5-yr period changes considerably from the 20-yr period since the extreme value extrapolation is made from a subset of the 20 years of storms. Even if the sampling of these storms were perfect, extreme values calculated from the different sets of storms would be different. The effect of sample length on extreme value predictions is very important, but outside the scope of this paper.

The situation improves if data from two satellites is included. Table 11 shows the results for 5 years of TSs sampled by *ERS-1* and Topex flying together. The cov's are about 30% smaller than in Table 9. A similar reduction is seen for the 20- and 90-yr periods. With 90 (20) years of data, the cov drops below 10% at a sampling region of about 150 km (400 km). Thus, it would take about 30–40 years of joint data from *ERS-1*/Topex to get a cov smaller than 10% using a sampling region of 200–300 km. Note that there are now three satellite altimeters flying so the error will decrease further, although we did quantify this case.

We found our results for TSs to be influenced by the storm decay scale, -0.38, in Eq. (4). This parameter controls how rapidly the winds decay as a function of distance from the storm center. According to Holland (1980), our value of -0.38 is a lower limit on the decay rate. Table 12 shows the result for a 20-yr period with double our original decay rate (-0.76), corresponding roughly to an upper limit. Note that the cov's have increased substantially for the satellite, although not much for the site. From this we conclude that the satellite cov's for TSs in Table 7 are on the optimistic side. The real answer will lie somewhere between Tables 7 and 12. Exactly where will depend on the local storm climatology.

Our analysis of TSs is based on Gulf of Mexico storms where the annual recurrence rate is about one storm per year. In some locations like the South China Sea near Taiwan, the storm occurrence rate will be much higher—up to four times the gulf. For these regions the cov's will be smaller than those given above. We can get a good estimate of the performance near Taiwan by simply assuming that the same number of storms in Table 7 occurred in a 5-yr period. For this case, the site cov drops by about a factor of 3, while the satellite cov for 300 km drops by about a factor of 2. We should remember, however, that five years of data gives a limited sample of the storm population that cannot include much of the year-to-year variability in storm characteristics.

4. Conclusions and recommendations

We have studied the effect of the gaps inherent in satellite wave data on the wave height extremes derived from that data. To do this, we set up a simple numerical experiment in which a series of parameterized storms were released and sampled by a simulated in situ instrument, and a satellite with realistic orbital characteristics. Sensor errors were assumed negligible — the only errors came from the space–time sampling constraints inherent to the measurement method. We considered both tropical and extratropical storms since they have different length and time scales, and often dominate extremes in many regions of interest to the oil industry.

TABLE 10. The 100-yr significant wave heights from five years of ETS simulations.

Region	Mean (m)	cov (%)	Combined (m)
Site	16.20	9.4	15.99
Sat 10	14.73	64.6	14.16
Sat 100	16.63	21.3	15.63
Sat 300	15.44	12.3	15.50
Sat 500	15.47	10.0	15.18

TABLE 12. The 100-yr significant wave heights from 20 years of TS simulations using decay rate twice that of Table 6.

Region	Mean (m)	cov (%)	Combined (m)
Site	11.95	15.8	11.93
Sat 10	16.26	99.7	16.49
Sat 100	13.29	48.2	12.89
Sat 300	12.18	18.4	12.44
Sat 500	11.84	11.6	11.95

Statistically stable results were obtained by sampling a large number of simulated storms. The simulated storms were based on simple parametric equations that preserve the time and space scales of real storms. The point of our simulations was not to estimate actual 100-yr wave heights, but to demonstrate how the uncertainty in extreme estimates depend on different data sources.

We ran two sets of simulations. Deterministic simulations with fixed severity but random path storms, showed that combining satellite measurements over a radius of 300 km around the site of interest gives equivalent information to hourly measurements at a site. Both site and satellite measurements give fewer measurements of TSs than ETSs because TSs have much smaller spatial scales. Results are essentially independent of whether we use Topex, Geosat, or ERS tracks.

The second set of simulations involved stochastic simulations with random tracks and variable severity. The 100-yr wave height was estimated by fitting a three-parameter Weibull distribution to the CDF of the measured wave heights. One of the main results of this study was to demonstrate that 100-yr wave heights can be estimated from satellite data using exactly the same CDF techniques that are used for measurements at a site. A CDF was calculated from all of the satellite measurements in an area surrounding the site of interest, an extreme value distribution was fit to the CDF, and the return-period wave height was picked off the distribution at the same probability level used for getting the wave height from site data.

We used the CDF method despite the fact that the peak-over-threshold (POT) method is generally preferred. The POT method fits an extreme value distribution to the largest significant wave height recorded in each storm. One advantage of POT over CDF is that POT is much more likely to satisfy the assumption that the data in the extreme value distribution are uncorrelated.

We did not use POT because it is not yet clear how to apply it to satellite data. Peaks from individual passes over a storm should be equivalent to peaks in a time series from a site, so the distribution function of peaks from a satellite should be the same as the distribution function for site data. It is, however, necessary to know the number of storms per year in order to calculate the probability level for the 100-yr wave height, and it is not immediately obvious how this number can be calculated from satellite data. It is possible that the number of storms could be calculated from our estimates of the fraction of storms measured by a satellite. If, for example, the satellite measured 23 storms with peak significant wave heights over 5 m, but the deterministic simulations indicated that it only sampled 25% of the storms, the probability level for the 100-yr wave height would be set as if 92 storms had actually occurred. We intend to study this possibility in future work.

The results of the stochastic calculations show that the cov for the 100-yr wave height in ETSs is less than 10% for 20 years of satellite measurements using a sampling radius of 300 km. This is comparable to the uncertainty in present design code (API 1993; DOE 1987), and high-quality model hindcasts (Khandekar et al. 1994; SWIM 1985). Therefore, we conclude that satellite estimates of extreme wave heights in ETSs will be useful in many cases.

Based on the good results for ETSs, we conclude that satellite data should be valuable in locations dominated by monsoons and swell since these tend to have even longer length and time scales than ETSs. Regions that fall into this category include West Africa, Indonesia, and Malaysia.

For TSs, the situation is not as bright. The uncertainty due to undersampling of TSs by both site measurements and a single satellite is larger than from a good hindcast model. With two simultaneous satellites, the uncertainty drops by roughly 30%, but it would still take about 30 years of data to get a cov of less than 10% using a sampling region of 200–300 km. At present, there is less than three years of multisatellite data, so for now, hindcasts are likely to remain the preferred method. In the longer term, satellites look promising and certainly are still useful in the near term for making preliminary estimates in many areas where in situ data is sparse and hindcasts are not available.

Regardless of storm type, one must keep in mind that the usefulness of satellite data can be seriously limited by the need to sample over a 200–300-km-radii region. This is primarily because many platforms lie within roughly 100 km of the coast where there will be substantial spatial gradients in the metocean climate. Sampling over 200–300 km in these regions will only work well if the gradients are linear. A similar problem will arise in regions where storm ''alleys'' may exist. Perhaps the best solution to this problem is to increase the number of satellites because our results show that satellite performance then improves substantially.

REFERENCES

API, 1993: *Recommended Practice for Planning, Designing, and Constructing Fixed Offshore Platforms.* American Petroleum Institute.

Carter, D. J. T., 1993: Estimating extreme wave heights in the NE Atlantic from GEOSAT data. Offshore Tech. Rep. OTH 93 396, Health and Safety Executive, London, United Kingdom.

——, P. G. Challenor, and M. A. Srokosz, 1992: An assessment of GEOSAT wave height and wind speed measurements. *J. Geophys. Res.,* **97,** 11 383–11 392.

Charriez, P., M. Olagnon, and J. Tournadre, 1992: Confidence intervals associated with satellite measurements of wave and wind environment. *Proc. 11th Int. Conf. on Offshore Mechanics and Arctic Engineering.* 313–320.

Chouinard, L. E., 1992: A statistical method for regional design wave heights in the Gulf of Mexico. *Proc. 24th Annual Offshore Technology Conf.,* Houston, TX.

Cooper, C. K., 1988: Parametric models of hurricane-generated winds, waves, and currents in deep water. *Proc. 24th Annual Offshore Technology Conf.,* Houston, TX.

Cotton, P. D., and D. J. T. Carter, 1994: Cross calibration of Topex, ERS-1, and GEOSAT wave heights. *J. Geophys. Res.,* **99,** 25 025–25 033.

Dobson, E. F., F. Monaldo, J. Goldhirsh, and J. Wilkerson, 1987: Validation of GEOSAT altimeter derived wind speeds and significant wave heights using buoy data. *Johns Hopkins APL Tech. Dig.,* **8,** 222–233.

DOE, 1987: Guidance notes for the design and construction of offshore installations. U.K. Dept. of Energy, London, United Kingdom.

Glazman, R. E., and S. H. Pilorz, 1990: Effects of sea maturity on satellite altimeter measurements. *J. Geophys. Res.,* **95,** 2857–2870.

Hogan, P. J., H. E. Hurlburt, G. Jacobs, A. J. Wallcraft, W. J. Teague, and J. L. Mitchell, 1992: Simulation of GEOSAT, Topex/Poseidon, and ERS-1 altimeter data from a 1/8 deg. Pacific Ocean model: Effects of space–time resolution on mesoscale sea surface height variability. *MTS J.,* **26,** 98–107.

Hogben, N., and F. E. Lumb, 1967: *Ocean Wave Statistics.* Her Majesty's Stationary Office.

Holland, G. J., 1980: An analytic model of the wind and pressure profiles in hurricanes. *Mon. Wea. Rev.,* **108,** 1212–1230.

Khandekar, M. L., and R. Lalbeharry, 1994: The performance of the Canadian spectral ocean wave model (CSOWM) during the Grand Banks ERS-1 SAR wave spectra validation experiment. *Atmos.–Ocean,* **32,** 31–60.

Kindle, J. C., 1986: Sampling strategies and model assimilation of altimetric data for ocean monitoring and prediction. *J. Geophys. Res.,* **91,** 2418–2432.

Lefevre, J. M., J. Barckicke, and Y. Ménard, 1994: A significant wave height dependent function for TOPEX/POSEIDON wind speed retrieval. *J. Geophys. Res.,* **99,** 25 035–25 049.

Mestas-Nunez, A. M., D. B. Chelton, M. H. Freilich, and J. G. Richman, 1994: An evaluation of ECMWF-based climatological wind stress fields. *J. Phys. Oceanogr.,* **24,** 1532–1549.

Peters, D. J., C. J. Shaw, C. K. Grant, J. C. Heideman, and D. Szabo, 1993: Modelling the North Sea through the North European storm study. *Proc. 24th Annual Offshore Tech. Conf.,* Houston, TX.

Stone and Webster Engineering Corp., 1978: Development and verification of a synthetic Northeaster model for coastal flood analysis. Final Rep. Federal Insur. Admin., Dept. Housing and Urban Dev.

SWIM Group, 1985: A shallow water intercomparison of three numerical wave prediction models (SWIM). *Quart. J. Roy. Meteor. Soc.,* **111,** 1087–1112.

Tournadre, J., and R. Ezraty, 1990: Local climatology of wind and sea state by means of satellite radar wave measurements. *J. Geophys. Res.,* **95,** 18 255–18 268.

Tucker, M. J., 1991: *Waves in Ocean Engineering.* Ellis Horwood.

Young, I. R., 1994: Global ocean wave statistics obtained from satellite observations. *Appl. Ocean Res.,* **16,** 235–248.